Excess Cohesive Particulate Matter Removal at Upflow Settling Conditions

Nazire Mazlum and Süleyman Mazlum
Engineering and Architecture Faculty, Environmental Engineering Dept. Süleyman Demirel University, Çünür Isparta 32260, Turkey

Mehmet Necdet Alpaslan
Engineering Faculty, Environmental Engineering Dept., Dokuz Eylül University, İzmir 35160, Turkey

DOI 10.1002/aic.11499
Published online June 4, 2008 in Wiley InterScience (www.interscience.wiley.com).

The magnitude of excess particulate matter separation from a flocculated suspension at upflow settling conditions was predicted from the concentration distribution of batch settling data. The settling data pairs were fitted to modified population-growth model. Settling surfaces at upflow operation were increased by inlaying pipes into the column and inclining it for 50°, 60°, 70 and 80° coinciding with 0.5563, 0.7152, 1.0455 and 2.0594 mm/s decreased surface hydraulic loading rates, respectively. The respective removal ratios observed at the applied loadings were 0.878, 0.848, 0.756 and 0.520, while the corresponding predicted efficiencies by mean value method were 0.865, 0.831, 0.773 and 0.512, respectively. It was demonstrated that removal predictions obtained from the batch settling tests were quite compatible with the observed removals of actual upflow operation. The investigation also demonstrated that concentration distribution of batch settling data heads successfully to predict the excess particulate matter removal at upflow settling. © 2008 American Institute of Chemical Engineers *AIChE J,* 54: 2045–2053, 2008

Keywords: cohesive solid particles, phase separation, batch settling, upflow settling, tilted settling surfaces

Introduction

Gravity settling refers to the common cost-effective phase-separation methods for solid particles from solid-liquid suspensions in industrial and environmental processes, i.e., in water and wastewater treatment plants. The particles in suspension are separated from the liquid phase depending on particles' physical properties,[1] and the forces induced on particles in suspension. Settling has been the subject to many researches for decades, and well delineated by a great deal of modeling studies.[2–24]

The solutions to mathematical modeling studies by numerical methods provide susceptible demonstrations to the problem. However, the broad variations in size, shape and density of the particles, as well as particle-particle interactions are the factors complicating the modeling of settling in solid-liquid suspensions.[18] It was stated[6] that articles presented on the modeling of continuous sedimentation disclose the fact that nonlinear nature of settling phenomena makes it necessary to include some *ad hoc* assumptions in the model to obtain a good fit of data. It was also stated that[25] the theory behind ideal sedimentation tanks assumes that the suspension moves in uniform flow, although numerous studies have shown numerous nonuniform flow patterns, which explains why the solid removal efficiency of real clarifiers does not match the theoretical predictions.

Correspondence concerning this article should be addressed to S. Mazlum at s.mazlum@mmf.sdu.edu.tr.

The development of simple mathematical approaches to sedimentation is of noteworthy interest to specialists in environmental technology.[12] An easily applicable approach was proposed for the determination of the surface area of the secondary settling tanks, based on a simplified solids-flux theory, of biological wastewater treatment facilities.[26] Another practical approach for one-dimension (1-D) modeling of continuous sedimentation, which considers the clarifier as a set of layers was also proposed.[13] The simplified layer model based on Kynch sedimentation theory,[27] which is known as solids-flux theory, has been largely put to use.[16]

The complex and interdependent separation mechanisms taking place in hindered settling columns need to be facilitated by mathematical approaches, to predict the separation for the given operational conditions with reasonable accuracy.[20] Batch settling tests provide the downward velocity of sludge/supernatant interface, and the performance of continuous-flow settlers is commonly predicted evaluating the batch settling data of the identical suspension.[28,9] Coe and Clevenger[29] were the first to establish the simple graphical technique to predict the susceptibility of full-scale continuous-flow settlers from batch tests.[12,23] However, it was claimed that[30] the design of continuous flow settlers for flocculated suspensions from batch settling data based on the supernatant-suspension discontinuity height is just approximate because the surface height of the sediment, building up the bottom of the cylinder, is not distinct, although some others claimed that settling layer in a settling column is distinct.[9]

It was also well reported that sedimentation tanks having increased settling surfaces provide enhanced settling on inclined surfaces, and the investigations well delineated the effective separation mechanisms from the solid-liquid phase.[9,10,31,32,33,34,35,36] In such a practice upflow velocity can easily be decreased, without decreasing influent flow rate, by inlaying tilted plates or tubes into the settling tanks.

The goal of this study was to present a lumped-parameter approach to predict the performance of the settling tanks at upflow operational conditions. The approach is based on the concentration distribution of the particulate matter, rather than the solid/liquid interphase, at batch settling conditions, because concentration distribution provides more accurate data as compared to descending solid/liquid interphase at batch settling tests. The excess removal at upflow conditions corresponds to the removal of particles of which settling rates are lower than the upflow velocity. In this study, it was deduced that the excess removal can be well predicted, processing the batch settling data by the mean value method,[37] where the excess removal is due to increased particle collisions in the flocculated conditions, resulting in adsorption of tiny particles on big particles and, additionally, mechanical filtration effects particularly effective in hindered settling region.

In the study, a mineral substance, bentonite clay, was selected to be tested as being cohesive solid particulate matter, because of its constant chemical composition and physical properties during the study. Additionally, as compared to the random nature of impurities encountered in natural water and wastewater environments, e.g., activated sludge suspended impurities, a clay material due to its constant characteristics all the time seemed the most appropriate cohesive material for this study. In the study, batch and flow tests were carried out in plastic cylindrical columns, being away from friction effects originating from both the wall roughness and column diameter. Flow tests were carried out at upflow conditions. The settling surfaces were increased by tilting the settling column in which a tubular module was also inlaid to multiply the settling surfaces. Particulate matter removals observed at flow tests were compared with the predictions obtained by the evaluation of the batch settling data.

Theoretical Considerations

Promotion of settling surfaces

The settling rate of a particle, v, in quiescent settling is given by Eq. 1

$$v = \frac{h}{t} \tag{1}$$

where h and t indicate the downward distance taken by the particle and time period for particle travel, respectively. In upflow conditions, settling rate of particles is decreased by the countercurrent flow velocity, S_0, as in Eq. 2

$$v - S_0 = \frac{h}{t} \tag{2}$$

where t indicates hydraulic retention time in the tank at flow. If the tank inner surfaces are increased by tilting, then upward velocity S_0, is decreased to S_0' as depicted in Figure 1; the figure demonstrates how the upflow velocity in a hollow cylindrical tube is decreased by tilting for three fictitious compartments where q represents the flow rate.

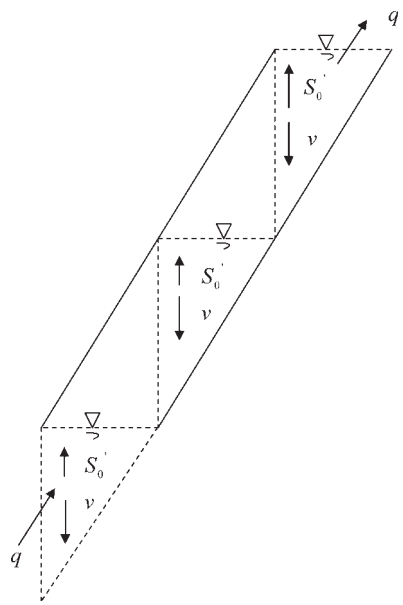

Figure 1. Three planar fictitious surfaces formed by tilting.

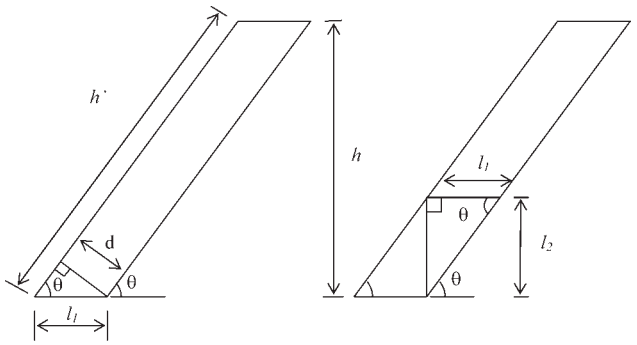

Figure 2. Presentation of geometrical relations in a tilted tube.

For the tilted-tube in Figure 1, Eq. 2 can be restated for the conditions having increased settling surfaces, or decreased upflow velocity (fictitious upflow velocity), as in Eq. 3

$$v - S_0' = \frac{h}{t} \tag{3}$$

where S_0' refers to decreased surface hydraulic loading rate in the tilted tube. Eq. 3 implies that inclination gives rise decreased surface hydraulic loading rate. Figure 2 sketches out how the surface hydraulic rate decreases by tilting.

In Figure 2, following geometrical relations can be written down

$$l_1 = \frac{d}{\sin\theta} \quad \text{and} \quad l_2 = l_1 . \tan\theta \tag{4}$$

The cross-sectional area of the tubes in a tilted position produces planar elliptical surfaces in vertical projection, having axes of d and l_1, for which the surface area can be restated as in Eq. 5

$$A = \pi . \frac{d}{2} . \frac{l_1}{2} \tag{5}$$

The vertical length of the tilted tube is

$$h = h' . \sin\theta \tag{6}$$

Then the number of elliptical surfaces m, formed in a tilted tube is

$$m = \frac{h}{b} \tag{7}$$

Resultant total settling surface area formed in a tilted tube is given as in Eq. 8

$$A' = m.A \tag{8}$$

Equation 8 can be rewritten as follows using Eqs. 4 to 7

$$A' = \frac{\pi}{4} . h' . d . \cos\theta \tag{9}$$

For a total number of tubes in a module, the total surface area formed is

$$\sum A = n' . A' \tag{10}$$

Mean value method

Mean value method foresees that if a function $f(x)$, is continuous (a, b) interval, where a denotes the origin, then $\bar{y}$ value existing in this interval (sec Figure 3) can be written down as in Eq.11,[38,39] where c indicates the point on y ordinate

$$\int_a^c f(y)dy = \bar{y} . (b - a) \tag{11}$$

in $\bar{y}$ which indicates the mean value. $\bar{y}$ can be singled out as follows

$$\bar{y} = \frac{1}{b - a} . \int_a^c f(y)dy \tag{12}$$

Above mathematical expressions suggest, in graphical terms, that the area A, in Figure 3a can be transformed to an equal area A, of a rectangular shape (Figure 3b), of which if the length is fixed to $a - b$ interval, then its height becomes $\bar{y}$, which is called the *mean value*. Figure 3c shows that once $\bar{y}$ is drawn, the areas on the left and right side of the inter-

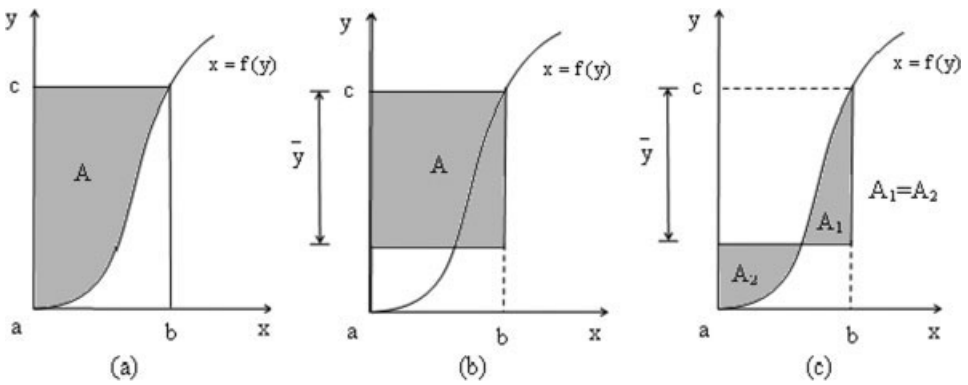

Figure 3. Mean value method for planar surfaces.

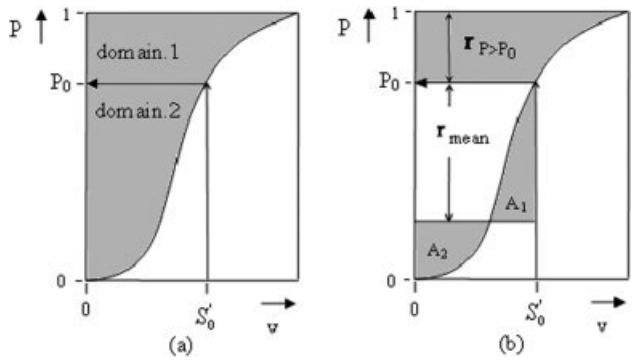

Figure 4. Evaluation of the settling rate distribution data of the particles in a suspension: (a) settling rates vs. particle percentages obtained at batch settling conditions; (b) method to predict the particle removal at flow conditions.

section of the crossing-curve become equal to each other ($A_1 = A_2$).

Prediction of settling efficiency

Particles in suspension can be designated within two groups at upflow settling: one stands for the particles having settling rates higher than fictitious upflow velocity, $v > S'_0$, and the other refers to the particles with settling rates lower than fictitious upflow velocity $v < S'_0$. While the former group of particles settle and separate from the suspension wholly, the latter are removed or separated only partially. Removal of particles of the latter type at upflow operation may be attributed to adsorption and mechanical filtration effects, of which the latter is particularly effective in hindered settling region.

For the settling rate distribution of the particles obtained at batch settling tests, two domains are considered as depicted in Figure 4: Domain. 1 represents the area for the particles having settling rates higher than S'_0 and domain. 2 refers to the particles which have settling rates lower than S'_0. Particles falling in domain. 1 settle wholly, while the particles in domain. 2 settle only partially. The removal ratios for the former and latter are shown as $r_{P>P_0}$ and r_{mean}, respectively as depicted in Figure 4.

Considering that frequency distribution curve in Figure 4 represents settling rate vs. particle removal percentage for a certain column depth at batch settling conditions, then total removal of particulate matter at upflow operation will be the summation of the removals in domain. 1 and domain. 2, as in Eq. 13

$$\sum r = r_{P>P_0} + r_{\text{mean}} \tag{13}$$

Replacing the removal ratio terms in Eq. 13 with the settling parameters, it takes the following form

$$\sum r = (1 - P_0) + \frac{1}{S'_0} \int_0^{P_0} v dP \tag{14}$$

The influent flow distribution and effluent weir hydraulic loading rate also largely influence the particle separation in flow tanks. The suspension is supposed to flow at rather quiescent flow conditions in the settling column for efficient separation efficiency. The uniform distribution of the influent to the cross-section of the column inlet, accompanied by uniform and satisfactorily low hydraulic weir-loading in the outlet, prevent flow short circuiting and resuspension of the settled particles back into the column. The weir hydraulic loading rate to prevent the resuspension of the settled particles was checked by the following criterion[40]

$$\frac{Q}{L_{\text{weir}}} < 5hS'_0 \tag{15}$$

where Q and L_{wier} indicate the applied flow rate and total length of straight weir in the column outlet, respectively.

Curve modeling

In the study, following curve estimation model was used to fit x and y variables into functional expressions, where α, β and γ represent the constants of the function

$$y = \alpha \left\{ \frac{1}{1 + \beta e^{-\gamma x}} - \frac{1}{1 + \beta} \right\} \tag{16}$$

α, β, and γ constants were determined by minimizing the sum of squares (SSR) between the observed and fitted data as in Eq. 17, harnessing *Solver* in Microsoft Office Excel software.

$$SSR = \sum_{i=1}^{n} (y_{\text{observed}} - y_{\text{fitted}})^2 \tag{17}$$

Material and Method

In this study, bentonite clay was used as a solid particulate test material, because of its flocculating properties. Addition-

Table 1. Composition of the Bentonite by XRF

Element (%)		Oxide (%)	
Al	9.371	Al_2O_3	17.706
Ba	0.122	BaO	0.136
Br	0.001	Br	0.001
Ca	1.626	CaO	2.275
Cl	0.345	Cl	0.345
Cr	0.018	Cr_2O_3	0.026
Cu	0.004	CuO	0.005
Fe	4.054	Fe_2O_3	5.796
Ga	0.002	Ga_2O_3	0.003
K	0.815	K_2O	0.982
Mg	2.376	MgO	3.940
Mn	0.044	MnO_2	0.070
Na	2.218	Na_2O	2.990
Nb	0.002	Nb_2O_5	0.003
Ni	0.017	NiO	0.022
O	48.242		
P	0.035	P_2O_5	0.081
Pb	0.006	PbO	0.006
Rb	0.008	Rb	0.008
S	0.627	SO_3	1.567
Si	29.522	SiO_2	63.157
Sr	0.030	SrO	0.036
Ti	0.480	TiO_2	0.801
Y	0.004	Y_2O_3	0.004
Zn	0.008	ZnO	0.010
Zr	0.021	ZrO_2	0.028

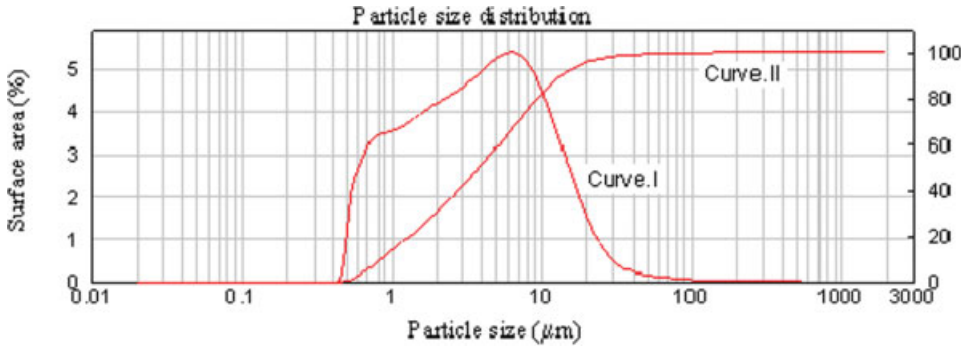

Figure 5. Size distribution of bentonite clay by laser diffraction method.

[Color figure can be viewed in the online issue, which is available at www.interscience.wiley.com.]

ally, the unchanging chemical composition and physical properties of the clay material were deemed supreme characteristics, as compared to other materials, particularly of organic origin, e.g., activated sludge biomass. Considering that the suspended impurities encountered in natural environments are inevitably inconsistant at each solid material supply, with rather nonuniform nature in due time, i.e., activated sludge biosolids, one with known and constant characteristics, as such "bentonite" was preferred as a test material to obtain compatible and consistent settling data.

X-ray diffractometer analysis (XRD PANalytical PR3040/60 X'Pert Pro, Philiphs) revealed that the major minerals existing in the tested clay material were quartz and montmorillonite. The composition determined by XRF analysis (Philips PW-2404 XRF) in Table 1 suggests that the clay is Na-Bentonite clay corroborating with the equivalencies of 96.437 *meq*Na^{+} and 81.300 *meq*Ca^{2+} for 100 g bentonite material.

Bentonite clay, supplied in fine powder form from a nearby cement factory, was heat-dried overnight at 105°C, and then dry density was determined to be 1,151 kg/m^3. The dry material was further sieved through 75 and 150 μm sized-sieves for 2 h, and the material in between these two sieves were used in the settling tests. Because clay materials have the tendency to agglomerate, the real grain-size distribution of the material by laser diffraction method (Malvern Mastersizer 2000) revealed that the effective size of the clay particles tested ranged from 0.45 to 100 μm as depicted in Figure 5: Curve.I depicts the particle-size distribution as a function of surface area of the bentonite material, and, Curve.II points out the cumulative frequency distribution.

Particulate matter concentrations in the suspension were measured by both the light-extinction principle in photometer (Pharmacia LKP NovaspecII), and by the gravimetric method, based on filtering the suspension through 0.45 μm cellulose-acetate membrane filter. Since clay is not opaque enough for reliable photometric readings, the raw clay material was dyed with methylen blue before its use in the settling tests. For dyeing, 10 g bentonite was introduced into 500 mL deionized water, and mixed until homogeneous suspension. Then 0.1 mg methylen blue was added into the suspension, in which dye dosage was 0.01 mg-methylen blue per *g*-dry clay. Next, pH of the suspension was adjusted to 8 and, subsequently, stirred in orbital incubator at 80°C for 4 h for permanent color formation. Following the stirring period, suspension was filtered and dewatered. The clay material was then transferred into 500 mL deionized water, and mixed until homogeneous suspension. This preparation was used as stock suspension. The feed suspensions were prepared in the reservoir by diluting the stock suspension in the feed reservoir with tap water to the predetermined concentration levels. During the test runs, the suspension in the reservoir was continuously aerated by diffused aeration to keep the suspension homogeneous. The settling tests were done at room-temperature conditions.

Batch settling tests were conducted in a cylindrical PVC column having 0.16 m inner dia. and 3 m vertical length. To sketch out the settling rate-concentration distribution with depth, samples were taken at certain time intervals from four separate sampling taps taking place at 0.5 m intervals from the top water surface.

Upflow settling tests were conducted in a cylindrical plexiglass column having 0.16 m inner dia. and 2.36 m length in vertical position. 17 PVC tubes, each having 0.02 m dia. and 0.65 m length, were inlaid into the column and fixed at the midpoint of the column. The settling surfaces were increased

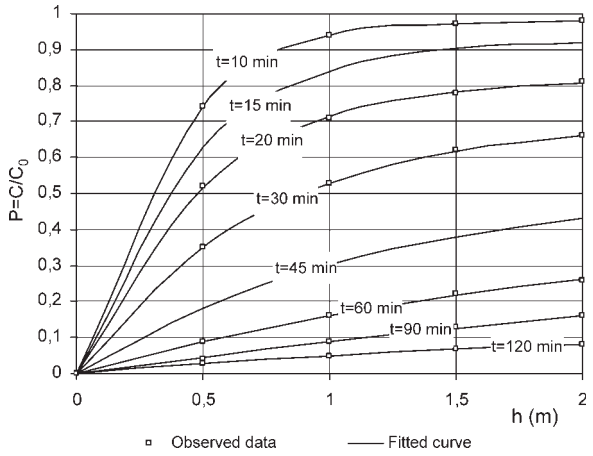

Figure 6. Nondimensional concentration distribution at batch settling conditions for 250 mg/L initial bentonite concentration and the curves fitted through Eq. 16.

Table 2. Fitted Curve Model Constants of Eq. 16 for the Curves in Figure 6

	t (min)							
Parameters	10	15	20	30	45	60	90	120
α	2.16604	4.63277	10.41023	10.40459	10.40228	10.40145	10.40069	10.40028
β	0.82445	0.24937	0.08551	0.07237	0.05285	0.04165	0.05558	0.01912
γ (1/m)	3.79140	2.59896	2.10097	1.45699	0.88932	0.50736	0.18379	0.30884
SSR	2.53E-06	9.94E-07	5.056E-06	1.309E-06	6.454E-07	2.099E-06	1.081E-05	2.177E-06

by column inclinations for 50°, 60°, 70° and 80°. The tests were carried out at inclined upflow operational conditions, where the inclinations gave rise to increased settling surfaces resulting in decreased surface hydraulic loading rates.

In upflow operation, the influent was fed into the column through the center of hopper-shaped inlet structure at the tank bottom and effluent was collected from the straight weir taking place along the diameter length of the column. The flow rate, weir length, and resultant weir loading rate were $1.388 \cdot 10^{-4}$ m^3/s, 0.16 m and $8.680 \cdot 10^{-4}$ $m^3/m.s$, respectively. The applied surface hydraulic loading rates at 50°, 60°, 70° and 80° tilted column operations were $5.562 \cdot 10^{-4}$, $7.151 \cdot 10^{-4}$, $1.045 \cdot 10^{-3}$ and $2.059 \cdot 10^{-3}$ m/s, respectively, which corresponded to 1.81, 2.04, 2.22 and 2.32 m water column heads.

Results

Batch settling

Batch settling of bentonite suspension having 250 mg/L initial concentration, was tested. Samples were withdrawn at 10, 15, 20, 30, 45, 60, 90 and 120th min from four separate sampling taps located at 0.5 m intervals along the column depth from the water surface, and the measured nondimensional particulate matter concentration distributions C/C_0 or P, were tabulated (data not shown). Then data pairs were fitted to the curve model given in Eq. 16, where y and x variables were replaced by P and h, respectively. Fitted curves are portrayed in Figure 6, and the accompanied model curve constants together with the coinciding sums of squares are given in Table 2.

The data depicted in Figure 6 display that initially relatively higher settling rates were observed as compared to later periods. The high-settling rates at earlier periods are due to relatively bigger size of the particles. The particles having relatively low-settling velocities keep suspended for longer periods.

Upflow operation

Upflow test runs were conducted at conditions having increased settling surfaces for 50°, 60°, 70° and 80° column inclinations. The influent was fed into the column in upflow direction from the bottom. In all the test runs, influent particulate matter concentration and flow rate were constant as 250 mg/L and 0.5 m^3/h. The effluent suspended solid concentrations obtained at steady-state operational conditions are given in Table 3. The columns in the table indicate inclination angle, water column head, total settling surface area, surface loading rate, effluent quality (suspended solids concentration) and suspended solids removal ratio, respectively.

Table 3. Operational and Quality Data at Upflow Test Runs

θ (°)	h (m)	A (m^2)	S'_0 (mm/s)	$C_{effluent}$ (mg/L)	$r_{observed}$
50	1.81	0.24965	0.5563	30.5	0.878
60	2.04	0.19420	0.7152	38	0.848
70	2.22	0.32840	1.0455	61	0.756
80	2.32	0.06744	2.0594	120	0.520

Prediction of Removal for Upflow Operation by Batch Settling Data

Data prediction and curve fitting

Since particulate matter removal efficiency in flocculated settling conditions changes with depth, water column head at batch settling tests should either reflect the water depth of continuous-flow tank or batch settling data need interpolation or extrapolation for the prediction of settling efficiency at flow conditions. Since the identical depths studied at upflow test runs were not covered at batch test, P-value coinciding with the depths at flow conditions were predicted first. The water column heads at upflow conditions for 50°, 60°, 70° and 80° inclinations were 1.81, 2.04, 2.22, 2.32 m, respectively, which were not the sampling depths at the batch settling test as can be seen in Figure 6. Then P-values corresponding to the aforementioned four depths were predicted for all the sampling periods depicted in Table 4 using the curve model parameters given in Table 2.

Next corresponding settling rates of the particles were computed. Successively predicted P, and computed v data pairs, given in Table 4, were fitted to curve model of Eq. 16 where y and x variables were replaced by P and v variables, respectively. The fitted curves and extracted model constants are given in Figure 7 and Table 5, respectively.

Table 4. Predicted P-Values for the Tested Flow Conditions

	P or C / C_0			
t (min)	$\theta = 50°$ $h = 1.81$ m	$\theta = 60°$ $h = 2.04$ m	$\theta = 70°$ $h = 2.22$ m	$\theta = 80°$ $h = 2.32$ m
10	0.9778	0.9787	0.9670	0.9516
15	0.9165	0.9190	0.9084	0.8946
20	0.8034	0.8096	0.8017	0.7897
30	0.6497	0.6611	0.6628	0.6606
45	0.4142	0.4325	0.4425	0.4462
60	0.2487	0.2618	0.2646	0.2625
90	0.1486	0.1618	0.1735	0.1812
120	0.0824	0.0907	0.0956	0.0975

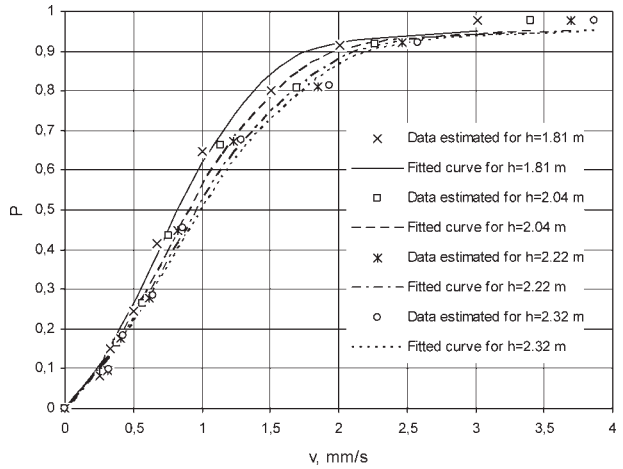

Figure 7. Fitted model curves through Eq. 16 concerning the studied depths at flow conditions.

Table 5. Fitted Curve Model Constants of Eq. 16 for the Curves in Figure 7

	h (mm)			
Parameters	1.81	2.04	2.22	2.32
α	1.10354	1.12417	1.14315	1.15490
β	6.33509	5.63466	5.10327	4.82050
γ *(1/m)*	2.67628	2.35543	2.13535	2.02359
SSR	0.000572	0.000557	0.000549	0.000545

Prediction of removal efficiency

Figure 8 portrays the data predicted utilizing batch settling data and the curves fitted to model equation (Eq. 16).

For the prediction of settling efficiency, Eq. 14 was harnessed in which *dP* was replaced with *v*-derivative of Eq. 16, as in Eq. 18

$$dP = \alpha \frac{\beta\gamma e^{-\gamma v}}{(1+\beta e^{-\gamma v})^2} dv \tag{18}$$

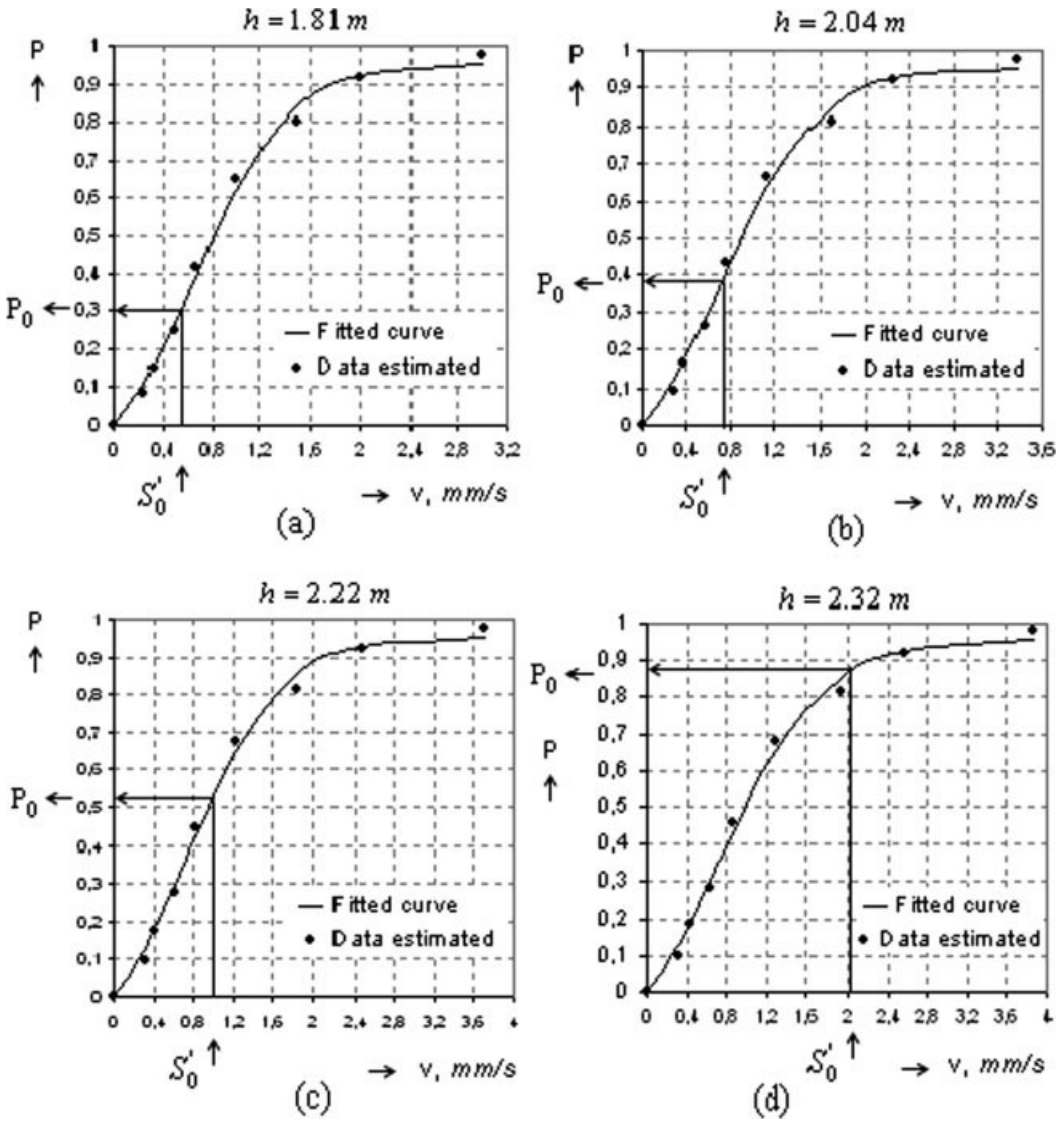

Figure 8. Distribution of particle settling and applied S'_0.

Table 6. Removal Predictions for Upflow Operational Conditions

Line Number	Parameters and/or Executed Operations	Experimental, Observed and Predicted Data			
1	θ (°)	50	60	70	80
2	h (m)	1.81	2.04	2.22	2.32
3	S_0' (mm/s)	0.5563	0.7152	1.0455	2.0594
4	P_0	0.3037	0.3801	0.5237	0.8762
5	$r_{P>P_0} = 1 - P_0$	0.6963	0.6199	0.4763	0.1238
6	$\int_0^{P_0} v\,dp = \int_0^{S_0'} \frac{\alpha\beta\gamma v e^{-\gamma v}}{(1+\beta e^{-\gamma v})^2}\,dv$	0.09431	0.15068	0.31072	0.79883
7	$r_{\text{mean}} = \frac{1}{S_0'}\int_0^{P_0} v\,dp = \frac{1}{S_0'}\int_0^{S_0'} \frac{\alpha\beta\gamma v e^{-\gamma v}}{(1+\beta e^{-\gamma v})^2}\,dv$	0.16953	0.21068	0.29719	0.38789
8	$r_{\text{predicted}} = r_{P>P_0} + r_{\text{mean}}$	0.866	0.831	0.773	0.512

P_0 values corresponding to the tested fictitious surface hydraulic loading rates S_0', can either be read from Figure 7, or can be predicted using model parameters given in Table 6. The tested S_0' values together with the corresponding P_0 values were tabulated in Table 6. The lines numbered 6 and 7 show the calculation results where the latter refers to the predicted excess removal due to upflow operational conditions.

Discussion and Conclusions

Solid particles in water environment have wide variations in size, shape and bulk densities. Furthermore, these physical properties are subject to continuous change for cohesive particles, which makes it impractical to calculate the particle's individual settling rates. However, although particle's individual settling rates in a suspension cannot be determined, settling rate distribution of the particles can easily be obtained in a batch column settling test and that concentration-time pair of data can be utilized to predict, to an extent, the particulate matter removal of the suspension in any tank at continuous-flow condition. Considering that in some suspensions where the sludge layer cannot be well distinguished from the liquid phase, the use of concentration distribution seems much helpful to be utilized rather than the use of declining insignificant liquid-sludge interphase.

Horizontal flow tanks are efficient for either discrete or flocculated settling if the inlet structure distributes the influent evenly to the tank cross-section at the entrance where the particles entering the tank at depths closer to the tank bottom, although they may have lower settling rates than upflow velocity, settle and separate from the suspension. However, it is well known that upflow conditions are not efficient for discrete settling, as compared to flocculent settling, because only the particles having settling rates higher than the upflow velocity settle and separate in upflow tanks. At upflow sedimentation, suspension enters the tank from the same plane at the bottom, and, hence, the inlet structure does not provide any advantage for any particles in the influent for early settling. Nevertheless, in flocculated conditions, particle interactions result in coalescence and growth, and the agglomerated particles settle with higher rates giving rise to high performance, which makes the upflow conditions more efficient for particle removal as compared to horizontal flow tanks.

The objective of the study was to predict the removal efficiency of cohesive particles of a suspension in a tank at upflow operational conditions. The mathematical approach used in this study implies that the prediction can be made basing upon batch settling data of the suspension. The approach assumes that:

1. Particles which have settling rates higher than the fictitious upflow velocity all settle and separate from the suspension.
2. Particles which have settling rates lower than the fictitious upflow velocity are only partially removed.

The removal of second group of particles (particles having settling rates lower than the fictitious upflow velocity) of a flocculated suspension at upflow settling conditions can be attributed to the increased agglomeration effects occurring under countercurrent flow conditions. Countercurrent flow conditions promote the efficiency of mechanical filtration, which is particularly effective in hindered settling region, where the increased collisions contribute to adsorption of tiny particles on the particle flocs. The adsorption effect is brought about by virtue of the cohesive nature of the particles, in which tiny particles collide and coalesce in countercurrent flow conditions (the influent flows upward while settling particles move downward), and, thus, reach high-settling rates (higher than the, fictitious, upflow velocity), and, consequently, settle and separate from the suspension.

In this study, the mean value method was employed to predict the removal efficiency of the particles of which settling rates are lower than the fictitious upflow velocity in the tank. Successful use of the method incorporating the mean value method, displayed that removal at upflow conditions can be well predicted basing upon (fictitious) surface hydraulic loading rate lumped-parameter at any operational conditions, i.e., for any tank geometry and hydraulic retention time, considering the inlet and outlet structures provide uniform flow distribution and collection.

The observed removal ratios at upflow conditions were 0.878, 0.848, 0.756, 0.520, as depicted in Table 3, and the respective predicted removals by batch settling data employing mean value method were 0.866, 0.831, 0.773 and 0.512 as outlined in Table 6. The success of the mean value method for the removal prediction demonstrated that fictitious upflow velocity, S_0', in Eq.14 is a favorable substitute for the upflow velocity, S_0, the former corresponds to the decreased (fictitious) surface hydraulic loading rate by inclination of inlaid tubes, and the latter corresponds to conventional column. For a column without promoted (increased) surfaces, fictitious upflow velocity (or decreased surface hydraulic loading rate) equals to upflow velocity (surface hydraulic loading rate).

Notation

v = particle settling velocity
h = vertical settling depth
t = settling time
S_0 = upflow velocity or surface hydraulic loading rate
S_0' = fictitious upflow velocity or decreased surface hydraulic loading rate
l_1, l_2 = geometric dimensions on the tube settler
d = diameter of the tube settler
A = cross-sectional area of the tube settler
h' = the length of the tube settler
θ = tube settler inclination angle
m = the number of elliptical surfaces in a single tube settler
n' = total number of elliptical surfaces in a settling column
P = the percentage of suspended solids removal
P_0 = the percentage of suspended solids removal corresponding to the applied surface hydraulic loading rate
Q = flow rate
r = particulate matter removal ratio (efficiency)
L_{weir} = weir length of the straight weir
SSR = sums of squares
C = suspended solid concentration
C_0 = initial suspended solid concentration

Greek letters

α,β,γ = model constants

Literature Cited

1. Addai-Mensah J, Ralston J. Interfacial chemistry and particle interactions and their impact upon the dewatering behaviour of iron oxide dispersions. *Hydrometallurgy*. 2004;74:221–231.
2. Chancelier JPh, Cohen D Lara M, Joannis C, Pacard F. New insights in dynamic modeling of a secondary settler-I. flux theory and steady-states analysis. *Water Res*. 1997;31(8):1847–1856.
3. Chancelier JPh, Cohen De Lara M, Joannis C, Pacard F. New insights in dynamic modeling of a secondary settler -II.Dynamic analyses. *Water Res.* 1997;31(8):1857–1866.
4. Deininger A, Holthausen E, Wilderer PA. Velocity and solids distribution in circular secondary clarifiers: Full scale measurements and numerical modelling. *Water Res*. 1998;32(10):2951–2958.
5. Bürger R, Concha F. Mathematical model and numerical simulation of the settling of flocculated suspensions. *Int J Multiphase Flow*. 1998;24(6):1005–1023.
6. Diehl S, Jeppsson ULF. A model of the settler coupled to the biological reactor. *Water Res*. 1998;32(2):31–342.
7. Thelen TV, Ramirez WF. Modeling of solid-siquid fluidization in the Stokes flow regime using two-phase flow theory. *AIChE J*. 1999;45(4):708–723.
8. Bürger R, Bustos MC, Concha F. Settling velocities of particulate systems: 9. Phenomenological theory of sedimentation processes: numerical simulation of the transient behaviour of flocculated suspensions in an ideal batch or continuous thickener. *Int J Min Proc.* 1999;55(4):67–282.
9. Latsa M, Assimacopoulos D, Stamou A, Markatos N. Two-phase modeling of batch sedimentation. *Appl Math Modeling*. 1999;23:881–897.
10. Stiles PJ, Kagan M. Convective sedimentation of colloidal particles in a bowl. *J Colloid and Interface Sci*. 1999;216:193–195.
11. Bürger R, Evje S, Karlsen KH, Lie KA. Numerical methods for the simulation of the settling of flocculated suspensions. *Chem Eng J*. 2000;80:91–104.
12. White DA, Verdone N. Numerical modeling of sedimentation process. *Chem Eng Sci*. 2000;5:2213–2222.
13. Chatellier P, Audic JM. A new model for wastewater treatment plant clarifier simulation. *Water Res.* 2000;34(2):690–693.
14. Lee SR, Kim YS, Kim YS. Analysis of sedimentation/consolidation method by finite element method. *Comp and Geotechnics*. 2000;27(2): 141–160.
15. Garrido P, Bürger R, Concha F. Settling velocities of particulate systems: 11. Comparison of phenomenological sedimentation-consolidation model with published experimental results. *Int J Min Proc*. 2000;60:213–227.
16. Wett B. A straight interpretation of the solids flux theory for a three-layer sedimentation model. *Water Res*. 2002;6(12):2949–2958.
17. Garrido P, Burgos R, Concha F, Bürger R. Software for the design and simulation of gravity thickeners. *Min Eng*. 2003;6(12):85–92.
18. Xue B, Sun Y. Modeling of sedimentation of polydisperse spherical beads with a broad size distribution. *Chem Eng Sci*. 2003;58(8):1531–1543.
19. Bürger R., Damasceno JJR, Karlsen KH. A mathematical model for batch and continuous thickening of flocculated suspensions in vessels with varying cross-section. *Int J Min Proc*. 2004;73(2–4):183–208.
20. Kim BH, Klima MS. Development and application of dynamic model for hindered-settling column separations. *Miner Eng*. 2004;17(3):403–410.
21. Ekama GA, Marais P. Assessing the applicability of the 1D flux theory to full-scale secondary settling tank design with a 2D hydrodynamic model. *Water Res*. 2004;38(3):495–506.
22. Nocon W. Mathematical modelling of distributed feed in continuous sedimentation. *Simul Mod Prac Theo*. 2006;14(5):493–505.
23. Tomkins MR, Baldock TE. Nielsen P. Hindered settling of sand grains. *Sedimentology*. 2005;52(6):1425–1432.
24. Nicholas AP, Walling DE, Sweet RJ, Fang X. New strategies for upscaling high-resolution flow and overbank sedimentation models to quantify floodplain sediment storage at the catchment scale. *J of Hydrology*. 2006;329(3–4):577–594.
25. Campbell BK, Jeff Empie H. Improving fluid flow in clarifiers using a highly porous media. *J Environ Eng*. 2006;132(10):1249–1254.
26. Sperling vM., Froes CMV. Determination of the required surface area for activated sludge final clarifiers based on a unified database. *Water Res*. 1999;33(8):1884–1894.
27. Kynch G J. A theory of sedimentation. *Trans Faraday Soc*. 1952: 48(166):166–176.
28. Lee HY, Oh JK, Lee DH. Interpretation of continuous settling behavior from batch settling data in a Versatic acid 10-water system. *Hydrometallurgy*. 1993;32(3):273–286.
29. Coe HS, Clevenger GH. Methods for determining the capacities of slime-settling tanks. *Trans A Inst Min Eng*. 1916;55:356–384.
30. Font R, Laveda ML. Semi-batch test of sedimentation. Application to design. *Chem Eng J*. 2000;80:157–165.
31. Kapoor B, Acrivos A. Sedimentation and sediment flow in settling tanks with inclined walls. *J Fluid Mech.* 1995;290:39–66.
32. Laux H, Ytrehus T. Computer simulation and experiments on two-phase flow in an inclined sedimentation vessel. *Powder Technol*. 1997;94(1):35–49.
33. Bandrowski J, Hehlmann J, Merta H, Ziolo J. Studies of sedimentation in settlers with packing. *Chem Eng Proc*. 1997;36:219–229.
34. Doron P, Simkhis M, Barnea D. Flow of solid-liquid mixtures in inclined pipes. *Int J Multiphase Flow*. 1997;23(2):313–323.
35. Chhabra RB, Ferreira JM. An analytical study of the motion of a sphere rolling down a smooth inclined plane in an incompressible Newtonian fluid. *Powder Technol*. 1999;104:130–138.
36. Ramadan A, Skalle P, Saasen A. Application of a three-layer modeling approach for solids transport in horizontal and inclined channels. *Chem Eng Sci*. 2005;60:2557–2570.
37. Mazlum N. Settling in tanks having increased surfaces. Süleyman Demirel University, Gradute School of Natural and Applied Sciences, 2007. PhD Thesis.
38. Piskunov N. Differential and Integral Calculus.Vol.1; (2nd edition), Moscow, Mir Publisher, Mackba; 1977.
39. Anton H, Bivens I, Davis S. *Calculus, Early Transcendentals*. John Wiley & Sons. Inc; 2005.
40. Huisman L. Sedimentation and Flotation. Mechanical Filtration: Lecture Notes. p 166. Delft University of Technology, Department of Civil Engineering, Division of Sanitary Engineering, Delft, The Netherlands; 1981.

Manuscript received Sept. 6, 2007, revision received Dec. 18, 2007, and final revision received Feb. 28, 2008.